PAPER • OPEN ACCESS

A theoretical study of the dynamical switching of a single spin by exchange forces

New Journal of Physics
The open access journal for physics

A theoretical study of the dynamical switching of a single spin by exchange forces

R Wieser[1,5], V Caciuc[2], C Lazo[3], H Hölscher[4], E Y Vedmedenko[1] and R Wiesendanger[1]

[1] Institut für Angewandte Physik, Universität Hamburg, D-20355 Hamburg, Germany
[2] Peter Grünberg Institut (PGI-1) and Institute for Advanced Simulation (IAS-1), Forschungszentrum Jülich and JARA, D-52425 Jülich, Germany
[3] Institut für Theoretische Physik und Astrophysik, Christian-Albrechts-Universität zu Kiel, D-24098 Kiel, Germany
[4] Institut für Mikrostrukturtechnik, Forschungszentrum Karlsruhe, PO Box 36 70, D-76021 Karlsruhe, Germany
E-mail: rwieser@physnet.uni-hamburg.de

New Journal of Physics **15** (2013) 013011 (16pp)
Received 4 October 2012
Published 9 January 2013
Online at http://www.njp.org/
doi:10.1088/1367-2630/15/1/013011

Abstract. We demonstrate the possibility of dynamically switching the spin of a single atom or molecule with the magnetic tip of an atomic force microscope making use of the acting exchange forces. We choose single V-, Nb- and Ta-benzene molecules as model systems and calculate the exchange interaction with an Fe tip using density functional theory. The exchange energy displays a Bethe–Slater-type behavior with ferromagnetic coupling at large tip–sample distance and antiferromagnetic coupling at closer proximity. The exchange energies reach maximum values of a few tens of meV, which allows one to switch single spins by overcoming the energy barrier due to the magneto-crystalline anisotropy. The spin dynamics of the system was explored by solving the time-dependent Schrödinger equation with additional Landau–Lifshitz-like spin relaxation. We find that the distance dependence of the exchange interaction

[5] Author to whom any correspondence should be addressed.

as well as the appearance of quantum tunneling results in different scenarios for the switching behavior, e.g. the tip can switch the adatom or lead to a stable superposition state with zero magnetization.

S Online supplementary data available from stacks.iop.org/NJP/15/013011/mmedia

Contents

1. Introduction

In the quest for smaller magnetic data storage devices, single magnetic atoms or molecular magnets on surfaces have recently come into the focus of experimental research as they constitute the ultimate limit of a single bit [1–4]. These studies have become possible using scanning probe microscopy, which allows one to measure the local properties of magnetic structures on the atomic level. The experimental challenge is to position the atoms or molecules controllably on a surface, to stabilize the magnetization against thermal fluctuations, to read the magnetic state and to switch between states. The first issue has been tackled with the aid of different experimental techniques such as atom manipulation with the tip of a scanning probe microscope [5] or by self-organization [6, 7]. The stability of the magnetization of the atom or molecule depends on the magneto-crystalline anisotropy, which provides a barrier between symmetry equivalent directions of the magnetization. So far, no system has been identified that allows one to manipulate a single magnetic moment in a controlled manner. Reading the magnetic state of a single atom or molecule, on the other hand, has recently been demonstrated both for single magnetic atoms [1, 5] and molecules [8, 9].

The final task is to switch the magnetization between different stable states. In principle, this can be realized by different means such as an external magnetic field, a spin-polarized current or the exchange coupling with a magnetic tip. An external field will lead to a switching scenario where all the atoms toggle. A spin-polarized scanning tunneling microscope (SP-STM) can be used to switch the magnetic moments with a current [10, 11]. While this method allows controllability on an atomic scale [12], it is restricted to conducting samples. On an insulating substrate, another method is therefore required and the natural choice is magnetic exchange force microscopy (MExFM) which has recently been demonstrated [13–15]. In such a setup, the magnetic tip directly interacts with the magnetic sample by the exchange interaction. The exchange forces decay rapidly with distance [16, 17] and therefore the tip needs to be brought into very close proximity to a single magnetic atom or molecule. The local character of the interaction should, in principle, allow one to monitor and switch the spin of a single atom [16, 17].

In this work, we use a combination of first-principles calculations and spin dynamics simulations to explore the feasibility of switching the spin of a single magnetic molecule due to the exchange forces with a magnetic tip in the dynamic mode of an MExFM. We have chosen a simple model system for our study which consists of an Fe tip composed of five atoms [15, 18] and magnetic half-sandwich vanadium-, niobium- and tantalum-benzene molecules. For simplicity, we have neglected the influence of the substrate on the molecule, as we are mainly interested in the direct interaction between the tip and the molecule. This class of transition-metal-benzene molecules has been theoretically investigated [19] and can be synthesized experimentally [20]. They provide a considerable magnetic moment as well as magneto-crystalline anisotropies of up to 7.5 meV per Ta-atom for Ta-benzene [19]. We find that the exchange forces are strong enough to overcome magneto-crystalline anisotropy barriers of a few meV per atom between different magnetization states. Apart from the question of how strong these tip–molecule magnetic forces are, whether they have a ferro-magnetic (FM) or antiferromagnetic (AFM) character and how they depend on the tip–sample separation distance, we also explore the possibility of manipulating the magnetization orientation of the molecule by means of exchange interaction with the AFM magnetic tip. To this end, we use spin dynamics simulations. We find different switching scenarios depending on the minimal tip–sample distance.

The paper is organized as follows. In the first part, we discuss the *ab initio* calculations of the exchange energies and forces. In the second part the distance-dependence and size of the exchange energy determined from first-principles are used to investigate the spin dynamics of a magnetic molecule interacting with a magnetic tip.

2. Exchange interaction between the tip and the molecule

The first-principles density functional theory (DFT) [21] calculations of the magnetic exchange forces between the tip and the molecule have been performed with the Vienna *ab initio* simulation package code [22, 23] using the projector augmented wave pseudopotentials [24] generated with the Perdew, Burke and Ernzerhof [25] exchange-correlation energy functional. The tip–molecule system was modeled by a tetragonal supercell of $14\times14\times20$ Å^3. The Kohn–Sham wave functions were expanded in a plane wave basis set with a cut-off energy of 500 eV and the k-mesh was sampled by the Γ-point only. Before treating the coupled tip–sample system, we performed separate structural relaxations of the Fe tip and the V-benzene, Nb-benzene and Ta-benzene molecules. No further structural relaxations were considered while approaching the tip to the molecule. However, for a starting FM and AFM alignment of the Fe tip and molecule magnetic moments, for each tip–molecule separation their magnetic moments were allowed to relax during the electronic self-consistency cycle. A schematic drawing of the tip–molecule configuration used in our study is illustrated in figure 1.

The calculated forces for the Fe tip per V-benzene system in an FM and AFM alignment between Fe and V magnetic moments are displayed in figure 2(a). One can note a significant difference between the forces calculated in the two configurations amounting to about 0.5 nN in a tip–molecule separation range between 3.2 and 3.5 Å. However, at a separation of 3 Å the two curves suddenly become identical. This surprising disappearance of the exchange force, which is the difference between the forces in the two alignments, for small tip–molecule distances, can be understood by looking at the magnetic moments of the Fe apex and V atoms. While the Fe and V moments in the AFM state, figure 2(b), remain nearly constant upon approaching the tip,

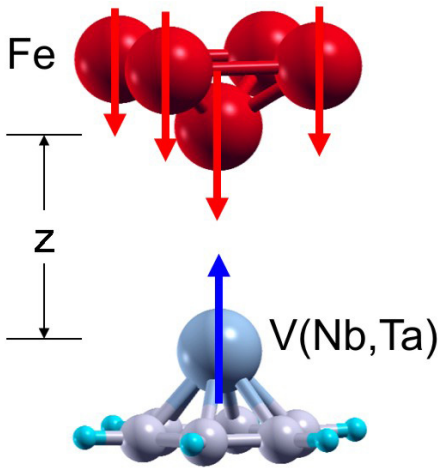

Figure 1. Setup of a magnetic Fe tip and a magnetic V-benzene molecule used in our study to evaluate the exchange interaction for parallel and anti-parallel alignment of the Fe tip and V magnetic moments. We also considered other TM-benzene half-sandwiches with niobium (Nb) and tantalum (Ta), which are the 4d- and 5d-elements isoelectronic to V, respectively.

there is a sudden jump in the FM state, figure 2(c), to an AFM alignment. This effect is due to the strong exchange interaction with the Fe tip which makes the FM alignment unstable and it converges into the AFM solution in our DFT calculation.

The exchange interaction between the tip and the molecule can be evaluated quantitatively by plotting the exchange energy which is the difference between the total energy of the FM and AFM solution $\Delta E(z) = E_{\mathrm{AFM}}(z) - E_{\mathrm{FM}}(z)$. Figure 2(d) shows that its absolute value rises rapidly at small tip–molecule separations and strongly favors the AFM configuration ($\Delta E < 0$). Interestingly, there is a change from a positive to a negative exchange energy indicating an FM coupling ($\Delta E > 0$) at large and an AFM coupling ($\Delta E < 0$) at small distances. This effect has been observed before in first-principles studies of the exchange interaction between a magnetic tip and a magnetic film or single magnetic atoms [16–18] and has been explained as a transition from an indirect to a direct exchange interaction. The curve also closely resembles the simple Bethe–Slater curve for the exchange interaction between single atoms. The size of the exchange energy rising up to 20 meV even at moderate separation ($\approx$4 Å) suggests the feasibility of overcoming the energy barrier due to magneto-crystalline anisotropy which separates different stable spin configurations of a magnetic molecule. The size of the exchange interaction across a vacuum gap has recently been measured [16] and agrees with first-principle calculations.

The difference between the forces in the two configurations constitutes the magnetic exchange force $F_{\mathrm{ex}}(z)$, i.e. $F_{\mathrm{ex}}(z) = F_{\mathrm{AFM}} - F_{\mathrm{FM}}$, which is the quantity measured in MExFM. In this way, MExFM allows one to image the magnetic structure of a surface on the atomic scale [13, 15]. Similar to the exchange energy, the exchange force shows a change of sign at a distance of about 4.2 Å. This is in accordance with the fact that the exchange force can be seen as the derivative of the exchange energy with tip–sample separation. Due to the large exchange forces in the intermediate-distance regime which are of the order reported in experimental MExFM studies [15, 16], it seems possible to detect the orientation of the magnetic moment of the V atom.

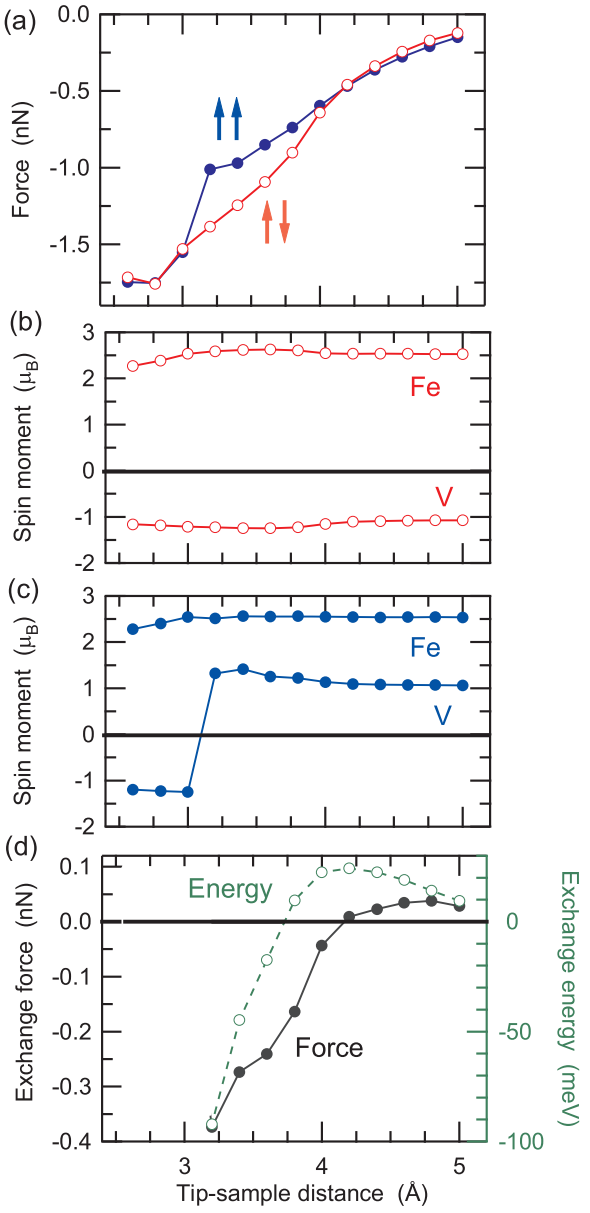

Figure 2. (a) The calculated z-component of the force between a vanadium-benzene molecule and an Fe tip in the FM and AFM starting configuration. The magnetic moments of the Fe apex and vanadium atoms for (b) an AFM and (c) an FM starting configuration. During the electronic self-consistency cycle, for each tip–molecule separation distance the magnetic moments of the tip–molecule system were allowed to relax. Therefore, in (c), the direction of the magnetic moment of V atoms switches when it is approached by the tip. (d) Exchange force and energy defined as the difference between the forces/energies in the AFM and FM configurations. Note that for a molecule–tip distance $d > 3.8$ Å, an FM configuration is in the ground state, whereas below this distance an AFM one is energetically more stable. Also starting from a separation distance $d = 3.0$ Å, a starting FM configuration relaxes to an AFM one.

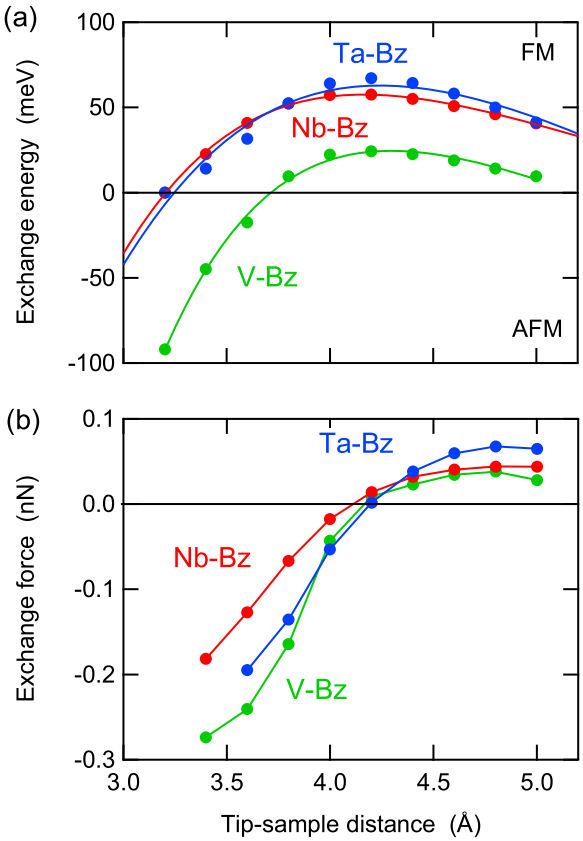

Figure 3. (a) Exchange energy between the Fe tip and benzene half-sandwich molecules with different TM atoms: V, Nb and Ta. Positive values denote a favorable FM configuration, while a negative sign indicates the AFM state to be energetically lower. (b) Exchange forces for the same systems.

In order to understand the influence of the magnetic transition metal (TM) atom on the strength and distance-dependence of the exchange energy, we have performed calculations for Nb- and Ta-benzene half-sandwiches. Nb and Ta are 4d- and 5d-TMs isoelectronic to V. The magnetic moment in these molecules amounts to 1 μ_B. Qualitatively, the exchange energy is similar to the case of V as seen in figure 3(a). However, the 4d-orbitals of Nb are significantly more extended than the 3d-orbitals of V, which leads to larger (positive) exchange energies and a shift of the crossing point to the AFM regime to smaller separations. Ta-benzene behaves quite similarly to Nb. The exchange forces for all three molecules are rather similar and the transition from positive to negative forces occurs at a similar distance. In conclusion, it seems that heavy 4d- and 5d-TMs are well suited to observe and switch the magnetic state of magnetic molecules, provided that these TMs carry a significant magnetic moment. Another important advantage of heavy 4d- and 5d-atoms is the dramatic increase of the magneto-crystalline anisotropy energy, which constitutes an energy barrier for the alignment of the magnetic moment and could allow for thermal stability of the magnetic moments at low temperatures. In the three cases the values are: 0.05 meV per V-benzene, 0.38 meV per Nb-benzene and 7.5 meV per Ta-benzene. For 5d-TM atoms on graphene, the enhancement of the magnetic anisotropy energy (MAE) is even

more dramatic and values of up to 50 meV per 5d-atom have been found in first-principle calculations [26].

We have further performed calculations for a sandwich structure composed of two benzene rings and one central vanadium atom, i.e. a benzene-V-benzene molecular structure. In this case, we found no splitting of the two force curves, due to the screening of the spin-polarized 3d-orbitals of the V atom by the second benzene ring.

We conclude from our first-principles calculations that one might experimentally detect and even switch the magnetic state of a magnetic molecule depending on the distance between the tip and the molecule. This process corresponds to the read and write procedure in a storage medium based on molecules. Similar exchange energy curves have been reported by Tao et al [17] for 3d TM atoms on Cu(001). While the exchange energies are large enough in our static DFT calculation to overcome the magneto-crystalline anisotropy barrier, the question of how a switching process can be observed in a dynamic MExFM experiment needs to be addressed by spin dynamics simulations.

3. Spin dynamics

So far we have addressed only static magnetic configurations. To prove the applicability to a real experiment it is necessary to perform additionally dynamical simulations. Therefore, we study as an example the dynamical response of the TM-benzene molecule, in the following V-benzene, disturbed by a magnetic tip, i.e. we use the distance-dependent exchange energy from figure 2. However, the given description is more general and can be used also for other atomic systems with adatoms, for instance 5d-TM adatoms on graphene which provide much larger magnetic anisotropy energies [26]. Or it can be used for Fe respectively Cu adatoms on the non-metallic Cu_2N surface [12]. From the experimental point of view there are different possible realizations to use exchange forces for magnetic switching or manipulation. In the following, we propose an experiment as realized in the MExFM [13]. In this case an oscillating tip is positioned above the molecule.

To realize such a kind of experiment in our simulations, we have considered a quantum mechanical Heisenberg model with magnetic properties that are well described by the Hamilton operator

$$\hat{\mathcal{H}} = -J(d)\,\mathbf{S}_\mathrm{t}\cdot\hat{\mathbf{S}}_\mathrm{s} - D_\mathrm{s}^x\left(\hat{S}_\mathrm{s}^x\right)^2 - D_\mathrm{s}^y\left(\hat{S}_\mathrm{s}^y\right)^2 - D_\mathrm{s}^z\left(\hat{S}_\mathrm{s}^z\right)^2. \tag{1}$$

The first term describes the exchange interaction between the tip and the sample coming from the *ab initio* calculations described before. The last terms are uniaxial anisotropies in the x-, y- and z-direction.

Due to the tip oscillation in the MExFM experiment the exchange interaction is time dependent: $d = d(t) \Rightarrow J(d) = J(t)$. The oscillation of the tip–sample distance is given by

$$d(t) = d_0 + A\cos(\omega t). \tag{2}$$

Here we assume a neutral position of the tip d_0 at 10 Å above the molecule. The oscillation amplitude A is assumed to be 5 Å respectively 6.5 Å, and $\omega = 2\pi f$, the oscillation frequency of the cantilever of the exchange force microscope, corresponds to time scales much larger than the relaxtion times of the spin dynamics.

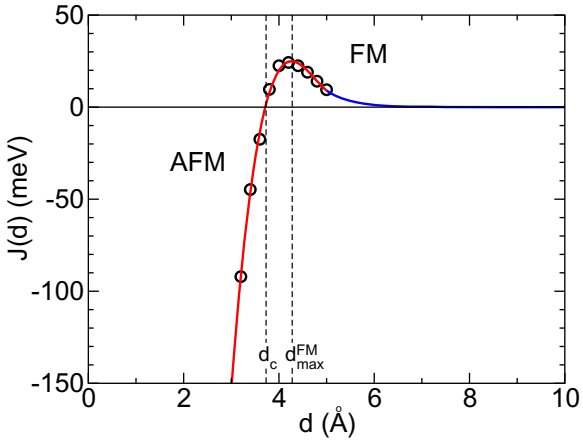

Figure 4. Distance dependence of the exchange constant J, which becomes negative (AFM) below $d_c = 3.75$ Å and has a maximum in the FM regime ($J > 0$) at $d^{\mathrm{FM}}_{\mathrm{max}}$. The points correspond to the *ab initio* calculations figure 2(d) and the solid lines are fitting curves.

Figure 4 shows the exchange constant $J(d)$ as a function of the tip–sample distance d. Here, we have assumed that the tip magnetization $\mathbf{S}_t$ as well as the spin operator $\hat{\mathbf{S}}_s$ are dimensionless ($\hbar \to 1$) and $J(d)$ has the dimension of energy.

The points correspond to the exchange energies given in figure 2(d) and the solid lines are fitting curves: we used a power law for $d \leqslant 5$ Å and assumed an exponential decay for $d > 5$ Å. d_c defines the separation at which $J(d)$ changes sign, i.e. transition from FM to AFM coupling. The form of this curve is not restricted to the case of V-benzene as it has been found also for other adatoms on a surface [17].

In our simulation, we further assume a stable tip polarization with magnetization direction given by the classical spin vector $\mathbf{S}_t$. Therefore, the exchange interaction acts as a time-dependent external field: $\hat{\mathcal{H}}_J = \mathbf{h}(t) \cdot \hat{\mathbf{S}}_s$, with $\mathbf{h}(t) = -J(d)\,\mathbf{S}_t$. In the following, we assume that the tip polarization is pointing downwards $\mathbf{S}_t = -\hat{\mathbf{z}}$.

In the following, we take the z-axis as the quantization axis and assume that this axis is an easy axis with $D^z_s = 0.05$ meV. The chosen value corresponds to a V-benzene molecule [19]. The value is very low from the experimental point of view and leads to an experimental temperature of a few milli-kelvin to avoid thermal instabilities. An experimentally more promising system is therefore 5d-TM atoms on graphene [26]. The values of the MAE are up to 1000 times higher in that system and in the range of 10–50 meV per 5d-TM atom. The corresponding experimental temperature is then in the range of a few kelvin.

For the x- and y-axis, we assume that $D^x_s = 0$ and $D^y_s = 0$ or, in the latter cases, $D^x_s = 0.01$ meV and $D^y_s = 0.06$ meV. After Landau [27] and Zener [28], quantum tunneling can be found in the latter case due to the additional off-diagonal elements in the Hamilton matrix. In the former case quantum tunneling is prohibited. We will show that in both cases interesting physics occurs.

The underlying equation of motion is the time-dependent Schrödinger equation (TDSE) with an additional relaxation term

$$\mathrm{i}\hbar \frac{\partial}{\partial t} |\psi\rangle = \hat{\mathcal{H}} |\psi\rangle - \mathrm{i}\lambda (\hat{\mathcal{H}} - \langle \hat{\mathcal{H}} \rangle) |\psi\rangle \,. \tag{3}$$

While the left-hand side and the first term on the right-hand side form the well-known TDSE, the second term on the right-hand side is an additional relaxation similar to the classical Landau–Lifshitz damping [29, 30] with a damping constant λ and $\langle\hat{\mathcal{H}}\rangle = \langle\psi|\,\hat{\mathcal{H}}\,|\psi\rangle$. Note that $|\psi\rangle = \sum_l c_l\,|\psi_l\rangle$ is a linear combination of the eigenstates $|\psi_l\rangle$ of an orthonormal basis. From figure 2, we expect a localized spin of $S = \frac{1}{2}$ for the V-benzene molecule. Therefore, uniaxial anisotropies along the quantization axis (z-axis) have no influence. However, the DFT calculations show a nonzero MAE along the direction of the quantization axis. Further, the V-benzene can be seen as an example of magnetic adatoms, e.g. 5d-TM atoms on graphene, with any spin quantum number S interacting with a magnetic tip. Therefore, to get a more general description and to take the effect of uniaxial anisotropies into account, we assume a system with $S = 1$. Therefore, our basis contains the following three states: $|1\rangle = |\uparrow\rangle$, $|0\rangle$ and $|-1\rangle = |\downarrow\rangle$. Such a spin system can be seen as a prototype for all systems with $S \geqslant 1$ as long as the dynamics is adiabatic. In these cases, only the crossing of the lowest energy states with $m_1^l = \pm S$ is important.

The eigenstates $|\psi_l\rangle$ are time independent; therefore the TDSE becomes a set of coupled differential equations for the expansion coefficients $c_l(t)$ which can be solved numerically. At the end, we are interested in the time dependence of the expectation values: $\langle\hat{S}_\mathrm{s}^\alpha\rangle = \langle\psi|\,\hat{S}_\mathrm{s}^\alpha\,|\psi\rangle$, $\alpha \in \{x, y, z\}$.

In the following, we discuss eight possible scenarios, defined by the occurrence of quantum tunneling, spin relaxation and the minimum tip–sample distance d_min. Let us start with the assumption that D_s^x and D_s^y vanish. This could be the case if the molecule feels no distortion due to the surface underneath. In this case tunneling of the magnetization is forbidden. We further assume a small energy relaxation due to electron-spin scattering processes and phonons. Now different situations occur depending on whether the tip–sample distance is larger or smaller than d_c, the distance where the exchange interaction changes from FM to AFM. In the former case, the exchange interaction is always FM, while in the latter case the exchange interaction changes during the oscillation period of the tip from FM to AFM and back to FM. Figure 5(a) shows the tip oscillation, the corresponding exchange interaction and the expectation value $\langle\hat{S}_\mathrm{s}^z\rangle$ of the molecular sample. In this case, the minimal tip–sample distance d_min is larger than d_c. In this scenario the exchange interaction leads to a controlled switching of the molecule if the initial tip–sample alignment was AFM. The situation changes if d_min becomes smaller than d_c as seen in figure 5(b). Here, we find a rectangular function like magnetization signal $\langle\hat{S}_\mathrm{s}^z\rangle$. This can be explained by the periodic change of the exchange interaction from FM to AFM and back to FM. Both scenarios can be found also within a classical description (see the supplementary data, available from stacks.iop.org/NJP/15/013011/mmedia) which can be used for single atoms with a strong hybridization with the underlying material [31, 32].

If we assume that D_s^x and/or D_s^y are nonzero, then quantum tunneling appears. In the following, we assume $D_\mathrm{s}^x = 0.01\,\mathrm{meV}$ and $D_\mathrm{s}^y = 0.06\,\mathrm{meV}$. Further, we assume a small relaxation with $\lambda = 0.01$. Again, we have to distinguish between the situations with d_min larger or smaller than d_c. Figure 6(a) shows the results for $d_\mathrm{min} > d_\mathrm{c}$. At the beginning the initial state was $|\psi\rangle = |\uparrow\rangle$ corresponding to $\langle\hat{S}_\mathrm{s}^z\rangle = 1$. Due to the fact that no external field has been taken into account and the initial exchange interaction is zero, both states $|\uparrow\rangle$ and $|\downarrow\rangle$ are energetically degenerate. The periodic oscillation of $\langle\hat{S}_\mathrm{s}^z\rangle$ between +1 and −1 (black area) is a direct consequence of a periodic tunneling between $|\uparrow\rangle$ and $|\downarrow\rangle$ at the zero field level crossing. With decreasing the tip–sample distance d the degeneracy between $|\uparrow\rangle$ and $|\downarrow\rangle$ is lifted

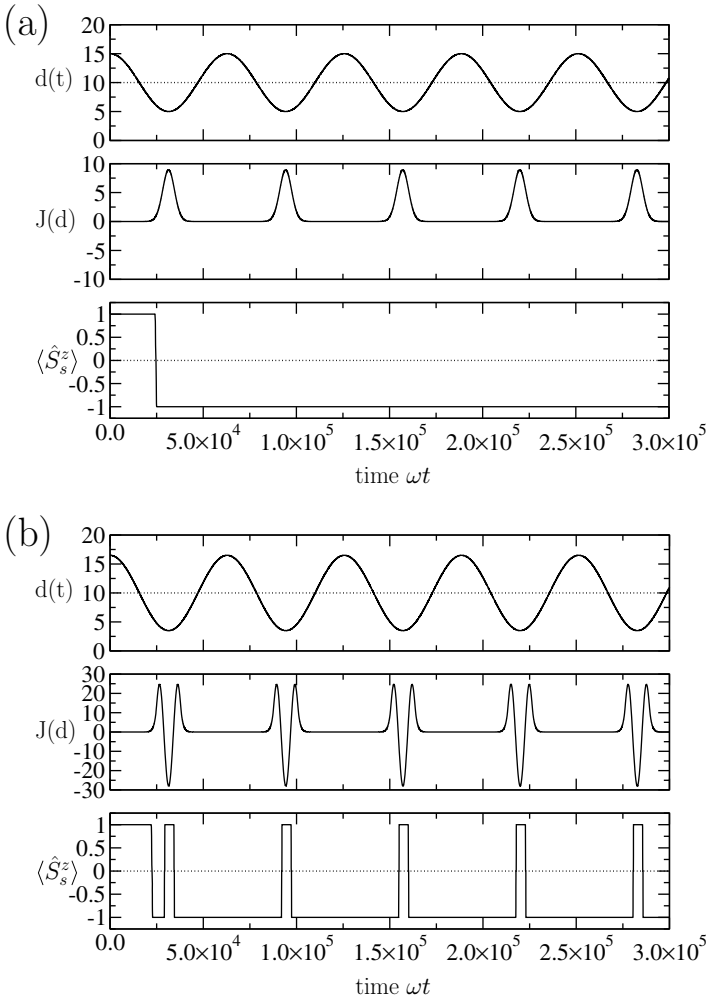

Figure 5. Tip–sample distance in $d(t)$ in Å, exchange interaction $J(d)$ in meV, and the quantum mechanical expectation value $\langle \hat{S}_s^z \rangle$ corresponding to the two scenarios with spin relaxation only $\left(\lambda = 0.01,\ D_s^x = D_s^y = 0\right)$, i.e. quantum tunneling is forbidden. (a) The first scenario: $A = 5$ Å; (b) the second scenario: $A = 6.5$ Å.

due to the exchange interaction and $|\psi\rangle$ becomes $|\psi\rangle = a\,|\uparrow\rangle + b\,|\downarrow\rangle$ with arbitrary a and b. Because of the additional relaxation, $\langle \hat{S}_s^z \rangle$ follows the effective field generated by the exchange interaction and becomes -1. As the tip retracts and the exchange interaction vanishes, $J(d) = 0$, $\langle \hat{S}_s^z \rangle$ becomes zero, corresponding to $|\psi\rangle = \frac{1}{\sqrt{2}}\left(|\uparrow\rangle \pm |\downarrow\rangle\right)$. This is a direct consequence of the interplay of quantum tunneling and relaxation. Note that $|0\rangle$ plays an unimportant role due to the fact that this state is higher in energy.

A similar situation occurs for $d_{\min} < d_c$. Figure 6(b) shows the corresponding simulation. The initial configuration is the same as before; therefore we see the same oscillation due to quantum tunneling at the beginning (black area). For nonzero exchange we find that $\langle \hat{S}_s^z \rangle$ follows the effective field and in between, for $J(d) = 0$, $\langle \hat{S}_s^z \rangle$ becomes zero corresponding to $|\psi\rangle = \frac{1}{\sqrt{2}}\left(|\uparrow\rangle \pm |\downarrow\rangle\right)$.

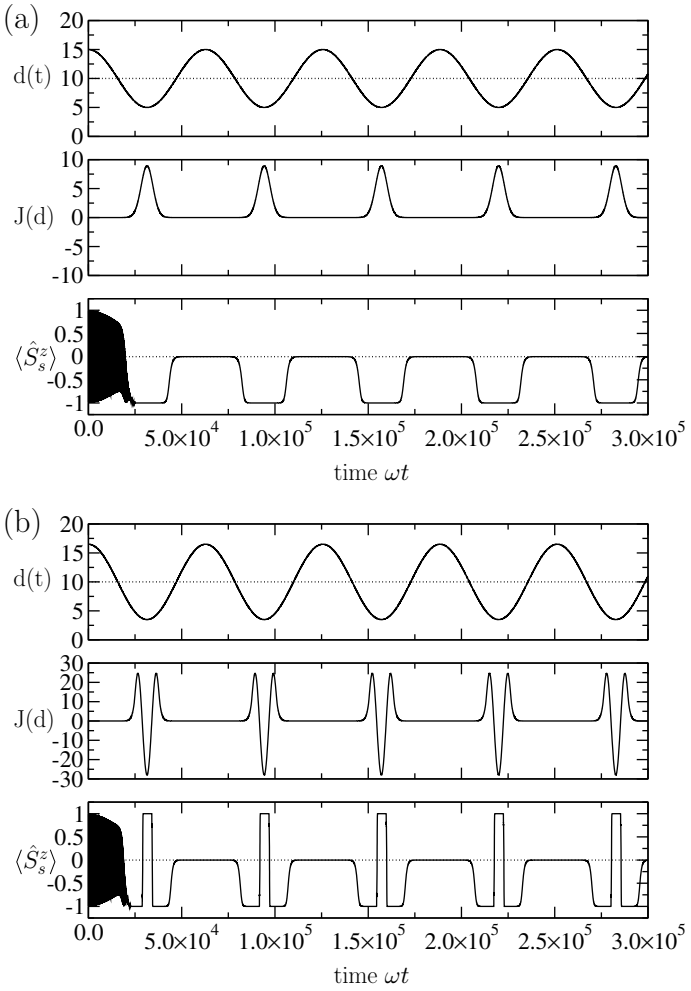

Figure 6. Tip–sample distance in $d(t)$ in Å, exchange interaction $J(d)$ in meV and the quantum mechanical expectation value $\langle \hat{S}_s^z \rangle$ corresponding to the two scenarios with relaxation ($\lambda = 0.01$) and quantum tunneling $\left(D_x = 0.01\,\text{meV}, D_y = 0.06\,\text{meV}\right)$. (a) The third scenario: $A = 5$ Å; (b) the fourth scenario: $A = 6.5$ Å. The black areas at the beginning of $\langle \hat{S}_s^z \rangle$ correspond to an oscillation between +1 and −1 caused by the periodic tunneling of $|\psi\rangle$ between its temporarily eigenstates $|\uparrow\rangle$ and $|\downarrow\rangle$.

To reinforce these predictions figure 7(a) shows the probabilities $P_\uparrow = \left|c_\uparrow\right|^2$ and $P_\downarrow = \left|c_\downarrow\right|^2$ corresponding to the third scenario (figure 6(a)). The oscillation of $\langle \hat{S}_s^z \rangle$ at the beginning can be clearly seen as oscillations of the probabilities $P_\uparrow$ and $P_\downarrow$. A zoom in (not shown) shows that there is a phase shift of $\pi/2$ between the oscillation of $P_\uparrow$ and $P_\downarrow$, which means that $|\psi\rangle$ oscillates between the eigenstates $|\uparrow\rangle$ and $|\downarrow\rangle$. After the first oscillation cycle a periodic change between 0 and 0.5 for $P_\uparrow$ and 0.5 and 1 for $P_\downarrow$ can be seen corresponding to a periodic change of $\langle \hat{S}_s^z \rangle$ between 0 and −1. From this signal it is quite simple to draw conclusions about $|\psi\rangle$, especially for $|\psi\rangle = |\uparrow\rangle$ or $|\psi\rangle = |\downarrow\rangle$. The states $|\psi\rangle_+ = \frac{1}{\sqrt{2}}(|\uparrow\rangle + |\downarrow\rangle)$ as well as $|\psi\rangle_- = \frac{1}{\sqrt{2}}(|\uparrow\rangle - |\downarrow\rangle)$ correspond to the probabilities $P_\uparrow = P_\downarrow = 0.5$. Therefore, we cannot say

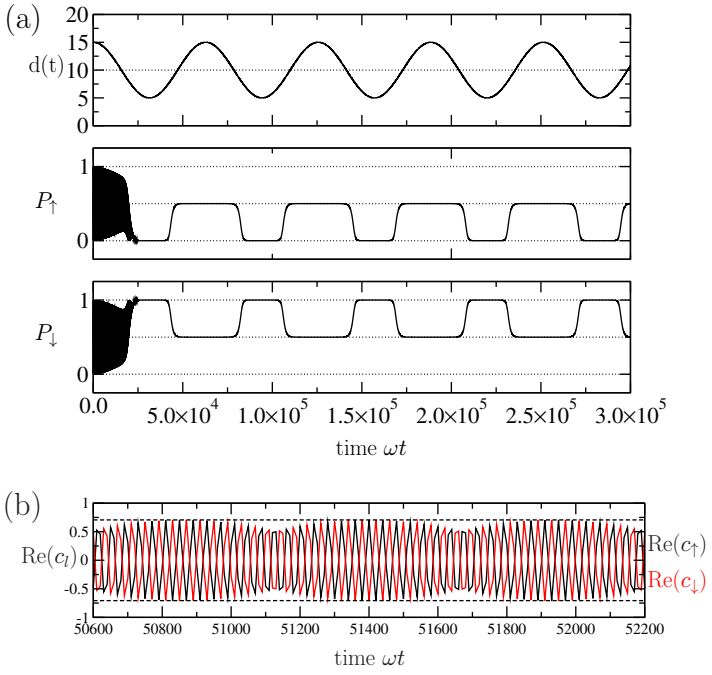

Figure 7. (a) Tip–sample distance and propabilities $P_\uparrow = |c_\uparrow|^2$ and $P_\downarrow = |c_\downarrow|^2$ corresponding to the third scenario. The black areas correspond to the oscillation of $|\psi\rangle$ between its eigenstates $|\uparrow\rangle$ and $|\downarrow\rangle$. (b) Real parts of the expansion coefficients $c_\uparrow$ and $c_\downarrow$ during the superposition state. The dashed lines correspond to $\pm 1/\sqrt{2}$.

from $P_\uparrow$ respectively $P_\downarrow$ if $|\psi\rangle_+$ or $|\psi\rangle_-$ appears. However, we can extract this information from $c_l = \mathrm{Re}(c_l) + \mathrm{i}\,\mathrm{Im}(c_l)$ $c_l \in \{c_\uparrow, c_\downarrow\}$. Figure 7(b) shows the real parts $\mathrm{Re}(c_\uparrow)$ and $\mathrm{Re}(c_\downarrow)$ as a function of time during which the superposition state occurs. The 180° phase shift corresponds to $|\psi\rangle_- = \frac{1}{\sqrt{2}}(|\uparrow\rangle - |\downarrow\rangle)$. Therefore, we can exclude $|\psi\rangle_+ = \frac{1}{\sqrt{2}}(|\uparrow\rangle + |\downarrow\rangle)$.

To explain these four scenarios and the following ones it is advantageous to give a schematic plot of the energy diagram of the eigenstates (see figure 8). This energy diagram is well known from the Landau–Zener transition [27, 28] to be a simplified sketch to explain the scenario. The dashed lines describe the diabatic states $|\uparrow\rangle$ and $|\downarrow\rangle$. The solid lines describe the adiabatic states $|\phi_\pm\rangle = \left[\left(E_J^\pm + h\right)|\uparrow\rangle + \Delta\,|\downarrow\rangle\right]/w_\pm$, with eigenenergies $E_J^\pm = \pm\sqrt{h^2 + \Delta^2}$, normalization $w_\pm = \sqrt{(E_J^\pm + h)^2 + \Delta^2}$ and splitting energy Δ; these states become equal to $|\uparrow\rangle$ respectively $|\downarrow\rangle$ in the limits of $h \to \pm\infty$. The adiabatic states only occur if quantum tunneling is allowed. In this case the diabatic states couple and split up. Δ describes the strength of the splitting.

In the first and the second scenario, tunneling is forbidden and the states $|\uparrow\rangle$ and $|\downarrow\rangle$ are uncoupled. Due to the relaxation the system tends to stay in the state with the lowest energy. For $J(d) = 0$ both states $|\uparrow\rangle$ and $|\downarrow\rangle$ are degenerate. The adatom remains in the last occupied state which has the lowest energy.

In the third and the fourth scenario the lowest energy state is $|\phi_-\rangle$. The initial configuration was $|\uparrow\rangle$. As long as $J(d) = 0$, $|\uparrow\rangle$ and $|\downarrow\rangle$ are energetically degenerated. Therefore, we see a periodic tunneling between both states. However, these states are higher in energy, therefore the

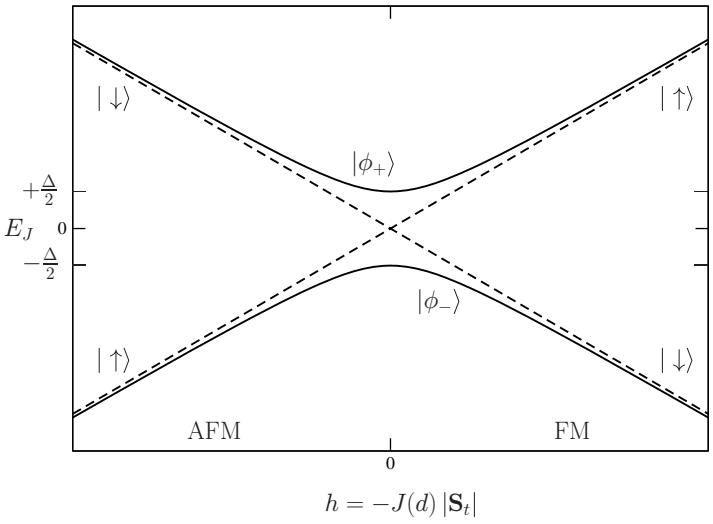

Figure 8. Exchange field h dependence of the eigenenergies E_J. The dashed lines describe the diabatic states $|\uparrow\rangle$ and $|\downarrow\rangle$ and the solid lines the adiabatic states $|\phi_\pm\rangle$.

system relaxes to the $|\phi_-\rangle$ state and stays there for the rest of the simulation. For $J(d) = 0$, $|\phi_-\rangle$ becomes $|\psi_-\rangle = \frac{1}{\sqrt{2}}(|\uparrow\rangle - |\downarrow\rangle)$. For $J(d) \to +\infty$, $|\phi_-\rangle$ becomes $|\downarrow\rangle$ due to the tip polarization which is assumed to be pointing in the $-\hat{\mathbf{z}}$-direction (downwards). For $J(d) \to -\infty$, $|\phi_-\rangle$ becomes $|\uparrow\rangle$. This can be seen in figures 6(a) and (b) during the FM respectively AFM exchange interaction between the tip and the molecule.

The last four scenarios appear if we assume that spin relaxation is prohibited ($\lambda = 0$); however, quantum tunneling appears $\left(D_x = 0.01\,\text{meV}, D_y = 0.06\,\text{meV}\right)$. These scenarios are related to the original Landau–Zener transition. Scenarios 5 ($d_{\min} < d_c$) and 6 ($d_{\min} > d_c$) appear if we assume that the initial configuration is the superposition state $|\psi_-\rangle = \frac{1}{\sqrt{2}}(|\uparrow\rangle - |\downarrow\rangle)$ which is identical to the adiabatic state $|\phi_-\rangle$. The system will stay in this adiabatic state due to the addiabaticity coming from the slow oscillation frequency. The corresponding magnetization curves $\langle\hat{S}_s^z\rangle$ are equal to figures 6(a) and (b), but without the fast oscillation at the beginning.

The situation changes if we assume the same initial configuration as before for scenarios 1–4. Here the system was prepared to be in the diabatic state $|\uparrow\rangle$. Figure 9(a) shows the situation with $d_{\min} > d_c$. In this case, $|\psi\rangle$ changes periodically between $|\uparrow\rangle$ and $|\downarrow\rangle$, for $J(d) = 0$ which can be seen as fast oscillation in $\langle\hat{S}_r^z\rangle$. For $J(d) \neq 0$, $\langle\hat{S}_s^z\rangle$ is equal to zero. The explanation therefore is simple and can be given with figure 8. For $J(d) = 0$, $E_J = 0$ and the system is at the crossing point between $|\uparrow\rangle$ and $|\downarrow\rangle$. Tunneling is allowed; therefore the system is periodically in $|\uparrow\rangle$ or $|\downarrow\rangle$. With increasing or decreasing $J(d)$ the energy splits and only one state $|\uparrow\rangle$ or $|\downarrow\rangle$ becomes energetically favorable. However, we assume no relaxation and E_J has to be conserved. To do so the system occupies the diabatic states $|\uparrow\rangle$ and $|\downarrow\rangle$ with 50% probability in the adiabatic limit. Therefore, we find that $\langle\hat{S}_s^z\rangle = 0$.

For $d_{\min} < d_c$ (the eighth scenario), we have additional zero crossings of $J(d)$ leading to two additional tunneling processes. It is known that the jumps in the magnetization strongly depend on the field sweeping rate [33, 34]. Due to the slow tip oscillation the system is in

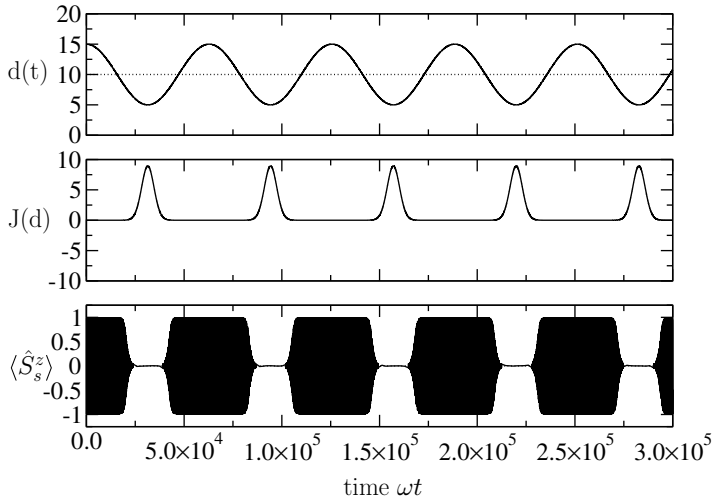

Figure 9. Tip–sample distance in $d(t)$ in Å, exchange interaction $J(d)$ in meV and the quantum mechanical expectation value $\langle \hat{S}_s^z \rangle$ corresponding to the scenarios with quantum tunneling $\left(D_x = 0.01\,\text{meV}, D_y = 0.06\,\text{meV}\right)$ but without spin relaxation ($\lambda = 0$): the seventh scenario ($A = 5$ Å). The black areas correspond to a fast but periodic oscillation.

the adiabatic limit; therefore scenario 8 is identical to scenario 7. For a faster oscillation (non-adiabatic regime) we can assume chaotic behavior.

4. Summary

With the aid of first-principles DFT calculations, we were able to calculate the force between a magnetic Fe tip and a TM-benzene molecule. Depending on parallel or antiparallel alignment of the tip and the adatom, we find a difference in the force between the tip and the molecule. This difference leads to a nonzero magnetic exchange force respectively exchange energy. The curve of the exchange energy shows a Bethe–Slater-like curve. Depending on the distance between the tip and the sample the interaction is either FM or AFM. This behavior seems to be universal and has been found for all the investigated TM atoms.

We could show that the assumed conditions play an important role. We have discussed eight different scenarios depending on the occurrence of relaxation and quantum tunneling. As a consequence of the Bethe–Slater-like exchange interaction and the minimal tip position d_{min}, we saw that a system without the appearance of quantum tunneling shows a controlled switching of the molecule from an antiparallel spin alignment of the tip and the sample (molecule) to a parallel one if the minimal tip–sample distance d_{min} is larger than the distance d_{c} where the FM exchange becomes AFM. If $d_{\text{min}} < d_{\text{c}}$ the molecule switches back to the antiparallel spin alignment caused by the changing exchange interaction.

The physics becomes more complicated if quantum tunneling plays a role. Caused by the degeneracy of $|\uparrow\rangle$ and $|\downarrow\rangle$ at zero field, a periodic tunneling appears for $J(d) = 0$. The exchange interaction $J(d)$ acts as an effective field and lifts this degeneracy. After the first oscillation cycle the molecule is in the state $|\psi\rangle = \frac{1}{\sqrt{2}}(|\uparrow\rangle - |\downarrow\rangle)$ if $J(d) = 0$ or follows the effective field coming from the exchange interaction.

The last four scenarios are under the assumption that relaxation is prohibited; however, quantum tunneling occurs. If the field sweep is slow enough, adiabatic Landau–Zener behavior can be found. Under the assumption that the initial state is equal to the adiabatic state $|\phi_-\rangle$ the adatom will stay in this state and an identical behavior as in scenarios 3 and 4 can be seen. If we assume the diabatic state $|\uparrow\rangle$ as the initial state the system shows a periodic tunneling between $|\uparrow\rangle$ and $|\downarrow\rangle$ without exchange interaction ($J(d) = 0$) and occupies both diabatic states with 50% probability. Corresponding to that, $\langle \hat{S}_s^z \rangle$ oscillates between ± 1 for $J(d) = 0$ and is equal to zero for $J(d) \neq 0$.

Our simulations have investigated the effect of the exchange interaction between the tip and the molecule. The description has been reduced to the interaction between the tip and the sample (molecule) to understand the occurring dynamics just from this interaction for the different scenarios described before. This means that we have given a general description of the scenarios which occur if there is exchange interaction between a magnetic tip and a magnetic adatom or molecule. This also means that we have neglected the effect coming from the temperature. This can be done under the assumption of a stable sample magnetization, without influence coming from the tip. This can be realized e.g. for adatoms on graphene in a cold environment. Additionally, as long as the temperature is low and the sample does not show a superparamagnetic behavior the temperature only assists the switching respectively tunneling process.

Further, in a real experiment we would also find dissipation effects like periodic changes of the magnetization or atomic configuration of the tip. This would also influence the oscillation amplitude of the cantilever. However, these effects are small disturbances with respect to the switching processes described in this paper. However, these effects are important to give detailed information on changes of the measuring signal, e.g. for MExFM, which are necessary to decide if the switching was successful or not without a second control measurement. Therefore, the next step in the theoretical consideration should be a self-consistent calculation taking these effects into account. Alternatively to the MExFM, such an experiment can be realized by a SP-STM scanning over the molecule without any current flow. However, problematic in this case could be that the STM is also able to manipulate the position of the atom and not only its magnetic moment.

Acknowledgments

This work was supported by the Deutsche Forschungsgemeinschaft (SFB 668 and HE 3292/7-1) and the Hamburg Cluster of Excellence NANOSPINTRONICS. The DFT calculations were performed at the Norddeutscher Verband Für Hoch- und Höchstleistungsrechnen (HLRN).

References

[1] Meier F, Zhou L, Wiebe J and Wiesendanger R 2008 *Science* **320** 82
[2] Gambardella P *et al* 2003 *Science* **300** 1130
[3] Hirjibehedin C F, Lutz C P and Heinrich A J 2006 *Science* **312** 102
[4] Hirjibehedin C F, Lin C-Y, Otte A F, Ternes M, Lutz C P, Jones B A and Heinrich A J 2007 *Science* **317** 1199
[5] Serrate D, Ferriani P, Yoshida Y, Hla S-W, Menzel M, von Bergmann K, Heinze S, Kubetzka A and Wiesendanger R 2010 *Nature Nanotechnol.* **5** 350

[6] Gambardella P, Dallmeyer A, Maiti K, Malagoli M C, Eberhardt W, Kern K and Carbone C 2002 *Nature* **416** 301
[7] Chylarecka D, Wäckerlin C, Kim T K, Müller K, Nolting F, Kleibert A, Ballav N and Jung T A 2010 *J. Phys. Chem. Lett.* **1** 1408
[8] Iacovita C, Rastei M V, Heinrich B W, Brumme T, Kortus J, Limot L and Bucher J P 2008 *Phys. Rev. Lett.* **101** 116602
[9] Brede J, Atodiresei N, Kuck S, Lazić P, Caciuc V, Morikawa Y, Hoffmann G, Blügel S and Wiesendanger R 2010 *Phys. Rev. Lett.* **105** 047204
[10] Krause S, Berbil-Bautista L, Herzog G, Bode M and Wiesendanger R 2007 *Science* **317** 1537
[11] Herzog G, Krause S and Wiesendanger R 2010 *Appl. Phys. Lett.* **96** 102505
[12] Loth S, von Bergmann K, Ternes M, Otte A F, Lutz C P and Heinrich A J 2010 *Nature Phys.* **6** 340
[13] Kaiser U, Schwarz A and Wiesendanger R 2007 *Nature* **446** 522
[14] Schwarz A, Kaiser U and Wiesendanger R 2009 *Nanotechnology* **20** 264017
[15] Schmidt R, Lazo C, Hölscher H, Pi U H, Caciuc V, Schwarz A, Wiesendanger R and Heinze S 2009 *Nano Lett.* **9** 200
[16] Schmidt R, Lazo C, Kaiser U, Schwarz A, Heinze S and Wiesendanger R 2011 *Phys. Rev. Lett.* **106** 257202
[17] Tao K, Stepanyuk V S, Hergert W, Rungger I, Sanvito S and Bruno P 2009 *Phys. Rev. Lett.* **103** 057202
[18] Lazo C, Caciuc V, Hölscher H and Heinze S 2008 *Phys. Rev.* B **78** 214416
[19] Mokrousov Y, Atodiresei N, Bihlmayer G, Heinze S and Blügel S 2007 *Nanotechnology* **18** 495402
[20] Weis P, Kemper P R and Bowers M T 1997 *J. Phys. Chem.* A **101** 8207
[21] Hohenberg P and Kohn W 1964 *Phys. Rev.* **136** B864
[22] Kresse G and Hafner J 1993 *Phys. Rev.* B **47** 558
[23] Kresse G and Furthmüller J 1996 *Phys. Rev.* B **54** 11169
[24] Blöchl P E 1994 *Phys. Rev.* B **50** 17953
[25] Perdew J P, Burke K and Ernzerhof M 1996 *Phys. Rev. Lett.* **77** 3865
[26] Zhang H, Lazo C, Blügel S, Heinze S and Mokrousov Y 2012 *Phys. Rev. Lett.* **108** 056802
[27] Landau D L 1932 *Phys. Z. Sowjetunion* **2** 46
[28] Zener C 1932 *Proc. R. Soc. Lond.* A **137** 696
[29] Gisin N 1981 *Helv. Phys. Acta* **54** 457
[30] Landau D L and Lifshitz E M 1935 *Phys. Z. Sowjetunion* **8** 153
[31] Gambardella P 2006 *Nature Mater.* **5** 431
[32] Khajetoorians A A, Lounis S, Chilian B, Costa A T, Zhou L, Mills D L, Wiebe J and Wiesendanger R 2011 *Phys. Rev. Lett.* **106** 037205
[33] García-Pablos D, García N and Raedt H D 1998 *J. Appl. Phys.* **83** 6937
[34] Rastelli E and Tassi A 2001 *Phys. Rev.* B **64** 064410